Supplementary materials for:

Estimation of forest canopy structure and understory light using spherical panorama images from smartphone photography

A. Z. Andis Arietta
Yale School of the Environment, Yale University, New Haven, CT, USA

Table S1. Effect of location on canopy measures estimated from standard DSLR HP images fit with OLS regression. N = 72 for all models.

Measure	Difference	95% C.I.	*p*
Canopy openness (%)	-2.48	-5.24, 0.28	0.08
Leaf area index	0.49	-0.05, 1.04	0.08
Global site factor	-3.06	-7.57, 1.45	0.19

Table S2. Regression coefficients and coefficients of determination from linear OLS regression models predicting canopy structure and light environment values for reference (standard DSLR HP) images from values for the same measure for comparison data sets. Intercepts that significantly deviate from 0 and slopes that significantly deviate from 1 at the alpha = 0.05 level are indicated in bold.

	Canopy openness (%)			LAI			GSF		
Image set	Intercept (95% C.I.)	Slope (95% C.I.)	R^2	Intercept (95% C.I.)	Slope (95% C.I.)	R^2	Intercept (95% C.I.)	Slope (95% C.I.)	R^2
$\text{Smartphone}_{\text{Full}}$	**-1.86 (-2.48, -1.24)**	**1.09 (1.02, 1.16)**	**0.93**	-0.6 (-1.32, 0.13)	**1.4 (1.19, 1.61)**	**0.71**	**-2.06 (-2.89, -1.22)**	1.06 (1, 1.13)	0.94
$\text{Smartphone}_{\text{Low}}$	**-1.69 (-2.32, -1.07)**	1.08 (1, 1.15)	0.92	-0.47 (-1.19, 0.25)	**1.35 (1.14, 1.55)**	**0.71**	**-1.86 (-2.7, -1.03)**	1.06 (0.99, 1.12)	0.94
$\text{Smartphone}_{\text{Fisheye}}$	**-2.39 (-3.28, -1.5)**	1.09 (0.99, 1.19)	0.87	-0.18 (-0.93, 0.58)	**1.38 (1.14, 1.61)**	**0.66**	**-2.86 (-4.05, -1.67)**	1.07 (0.98, 1.16)	0.89
$\text{DSLR}_{\text{Exp -5}}$	**4.21 (2.82, 5.61)**	0.84 (0.45, 1.23)	0.2	**3.2 (2.58, 3.83)**	**0.09 0.04, 0.14)**	**0.14**	**6.34 (4.09, 8.58)**	0.84 (0.44, 1.24)	0.19
$\text{DSLR}_{\text{Exp -4}}$	**3.58 (2.07, 5.1)**	0.84 (0.47, 1.22)	0.22	**3.37 (2.83, 3.9)**	**0.09 (0.04, 0.15)**	**0.14**	**5.35 (2.98, 7.72)**	0.86 (0.49, 1.23)	0.23
$\text{DSLR}_{\text{Exp -3}}$	**1.64 (1.34, 1.95)**	1.02 (0.97, 1.06)	0.97	**2.91 (2.49, 3.33)**	**0.19 (0.13, 0.24)**	**0.4**	**2.49 (2.02, 2.97)**	1 (0.96, 1.04)	0.97
$\text{DSLR}_{\text{Exp -2}}$	**1.34 (1.1, 1.59)**	1.02 (0.99, 1.06)	0.98	**1.45 (1.06, 1.84)**	**0.5 (0.43, 0.57)**	**0.76**	**1.95 (1.64, 2.27)**	1.01 (0.98, 1.04)	0.99
$\text{DSLR}_{\text{Exp -1}}$	**0.7 (0.56, 0.85)**	1.02 (1, 1.04)	0.99	0.8 (0.51, 1.08)	**0.71 (0.66, 0.77)**	**0.9**	1.05 (0.85, 1.24)	1.01 (1, 1.03)	1
$\text{DSLR}_{\text{Exp +1}}$	**-1.09 (-1.28, -0.89)**	**0.97 (0.94, 0.99)**	**0.99**	**-0.28 (-0.46, -0.11)**	**1.23 (1.19, 1.28)**	**0.97**	**-1.59 (-1.84, -1.35)**	**0.97 (0.96, 0.99)**	**0.99**
$\text{DSLR}_{\text{Exp +2}}$	**-2.2 (-2.65, -1.76)**	**0.88 (0.84, 0.92)**	**0.96**	-0.25 (-0.57, 0.06)	**1.42 (1.33, 1.52)**	**0.92**	**-3.42 (-4.01, -2.83)**	**0.91 (0.87, 0.95)**	**0.97**
$\text{DSLR}_{\text{Exp +3}}$	**-3.41 (-4.2, -2.63)**	**0.77 (0.71, 0.83)**	**0.91**	0.13 (-0.3, 0.55)	**1.55 (1.4, 1.71)**	**0.85**	**-5.4 (-6.52, -4.36)**	**0.82 (0.76, 0.87)**	**0.92**
$\text{DSLR}_{\text{Exp +4}}$	-0.95 (-2.47, 0.56)	**0.42 (0.34, 0.5)**	**0.61**	**0.59 (0.11, 1.06)**	**1.64 (1.43, 1.85)**	**0.78**	**-5.09 (-7.31, -2.86)**	**0.61 (0.52, 0.7)**	**0.73**
$\text{DSLR}_{\text{Exp +5}}$	-0.51 (-1.79, 0.76)	**0.28 (0.24, 0.33)**	**0.67**	**1.29 (0.84, 1.74)**	**1.61 (1.37, 1.84)**	**0.72**	**-4.37 (-6.68, -2.05)**	**0.44 (0.37, 0.51)**	**0.7**

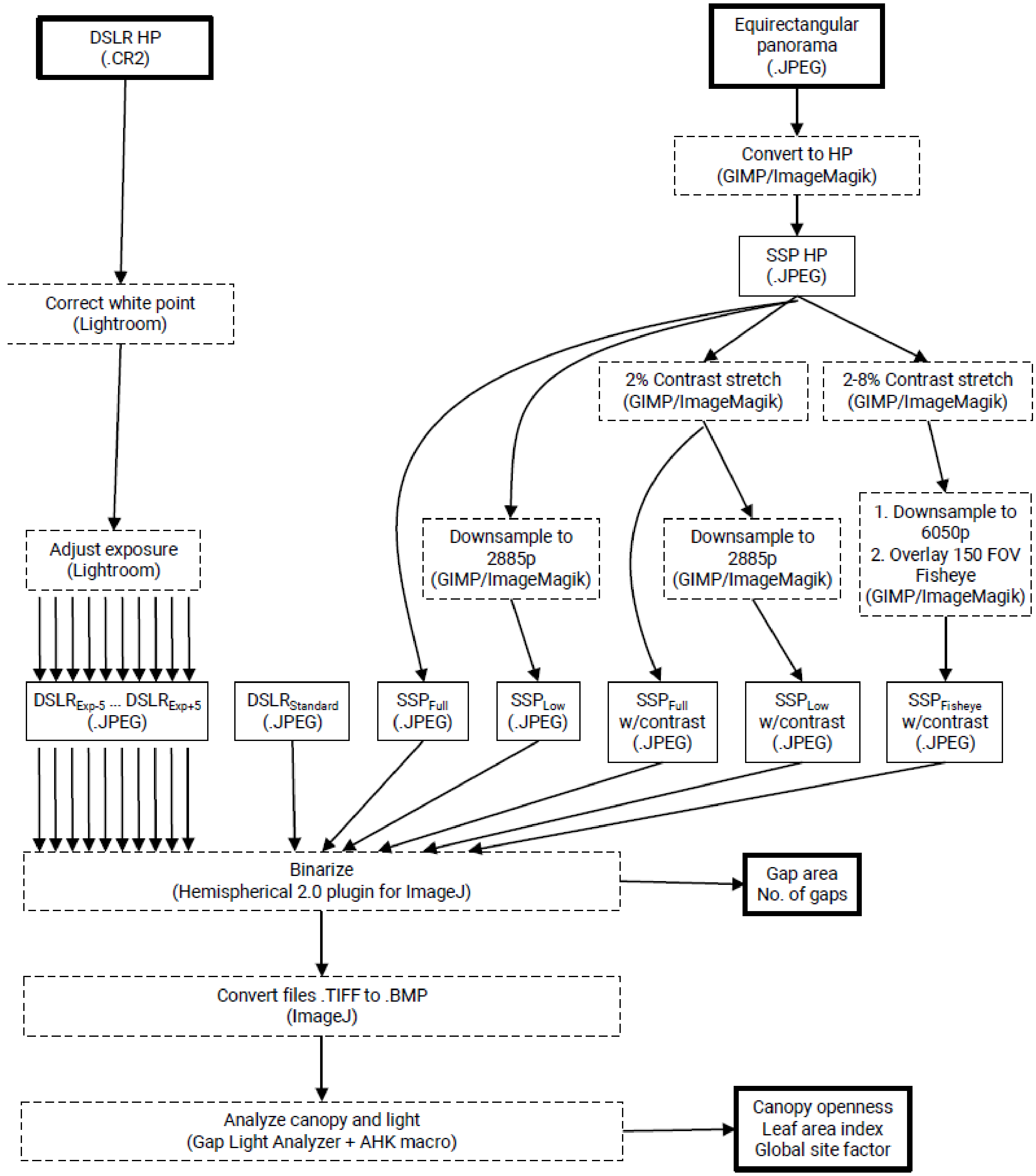

Figure S1. Workflow diagram for processing and analyzing hemispherical photos in this study. Intermediate files are indicated by solid boxes with file type in parentheses. Processing steps are indicated by dotted line boxes with the software required for the step in parentheses. Inputs and outputs are indicated with bold black boxes.

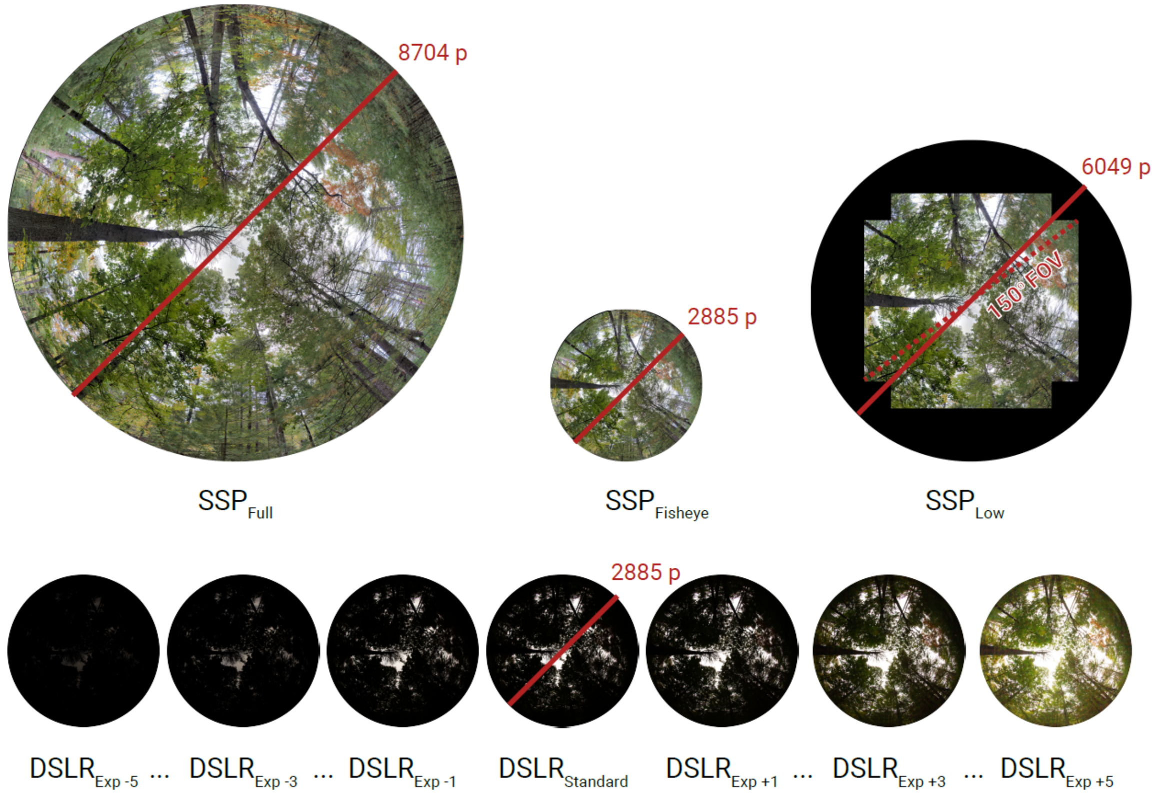

Figure S2. Comparison of the outputs following image processing for the same site. All images are scaled to relative size and pixel width of the diameter of the circular image is shown in red. Images in the top row were developed from smartphone spherical panoramas in full resolution (SSP_{Full}) or downsampled (SSP_{Low}) to the same resolution of DSLR images. Smartphone spherical panoramas were used to simulate the method proposed in Bianchi et al. (2017) ($SSP_{Fisheye}$) wherein a clip-on fisheye lens with 150 degree field-of-view attached to a smartphone was used to take perpendicular canopy images and merged into a partial hemispherical image. Image in the bottom row were acquired with a DSLR camera with a hemispherical lens and developed with standard protocols ($DSLR_{Standard}$). In order to compare relative impacts of incorrect exposure, DSLR images were over- or under-exposed by 1, 2, 3, 4, or 5 stops ($DSLR_{Exp\ -5}$ to $DSLR_{Exp\ +5}$).

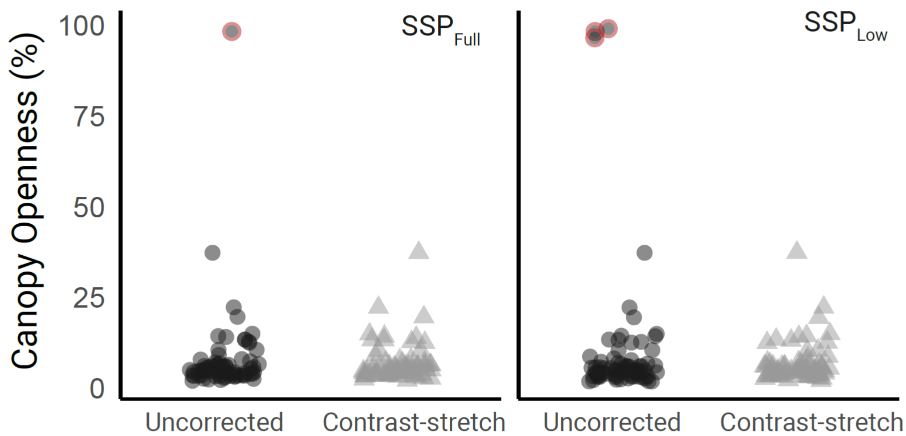

Figure S3. A small number of hemispherical images generated from smartphone spherical panoramas were incorrectly binarized by the thresholding algorithm (points indicated in red). This problem was more prevalent in the down-scaled images (SSP$_{Low}$) than the full resolution images (SSP$_{Full}$). Increasing the contrast of the images by 2% prior to binarization solved the problem.

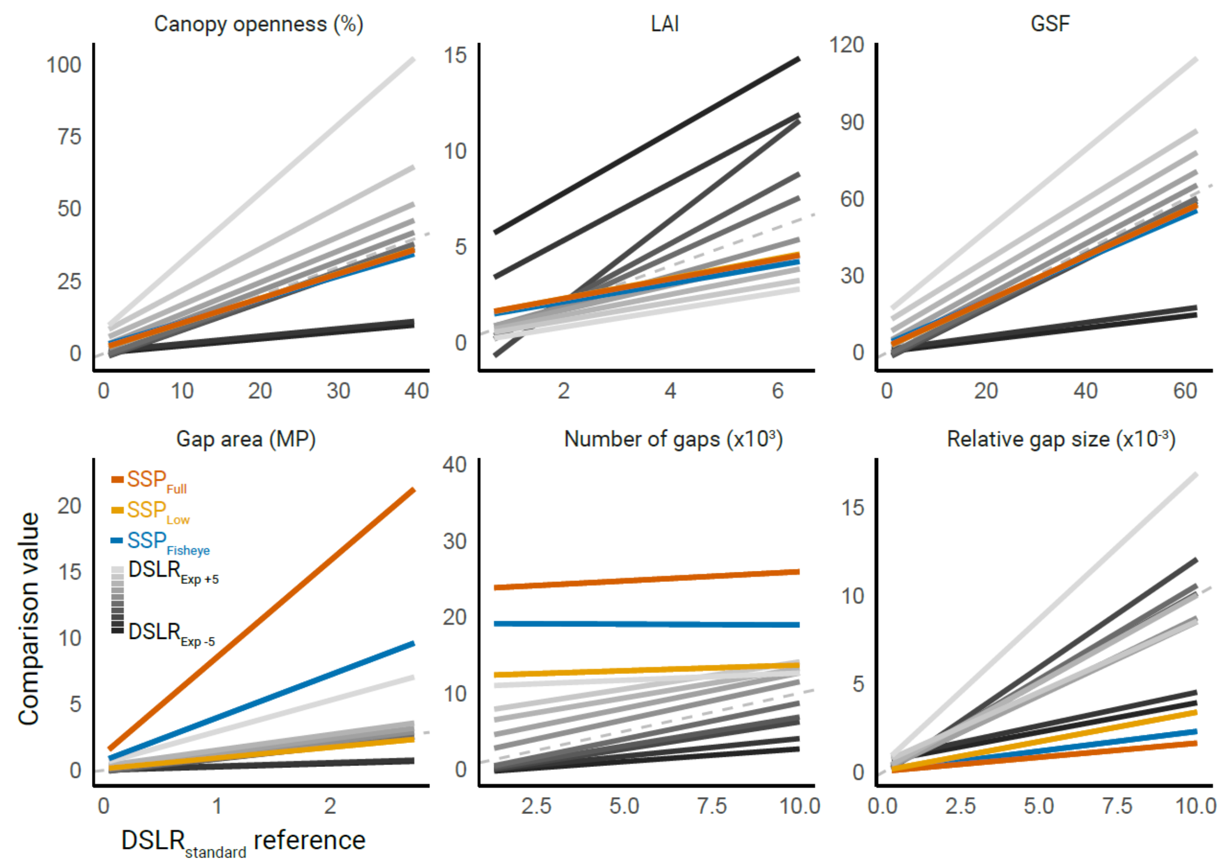

Figure S4. Linear regression estimates comparing three canopy structure metrics (canopy openness, leaf-area index (LAI), and global site factor (GSF)) and three image quality metrics (total gap area, number of gaps, and relative gap size) from images hemispherical images extracted from smartphone spherical panoramas (SSP) to those acquired with traditional DSLR camera and hemispherical lens ($DSLR_{Standard}$). Three processing methods for SSP hemispherical images were compared, including full resolution (SSP_{Full}, dark orange), images down-sampled to match the resolution of DSLR images (SSP_{Low}, light orange), and images simulated to approximate Bianchi et al.'s (2017) method using a smartphone and clip-on fisheye lens ($SSP_{Fisheye}$, blue) are shown. Estimates from DSLR images over- or under-exposed by -5 to 5 stops are shown for comparison. The 1:1 line is indicated by a dashed grey line.

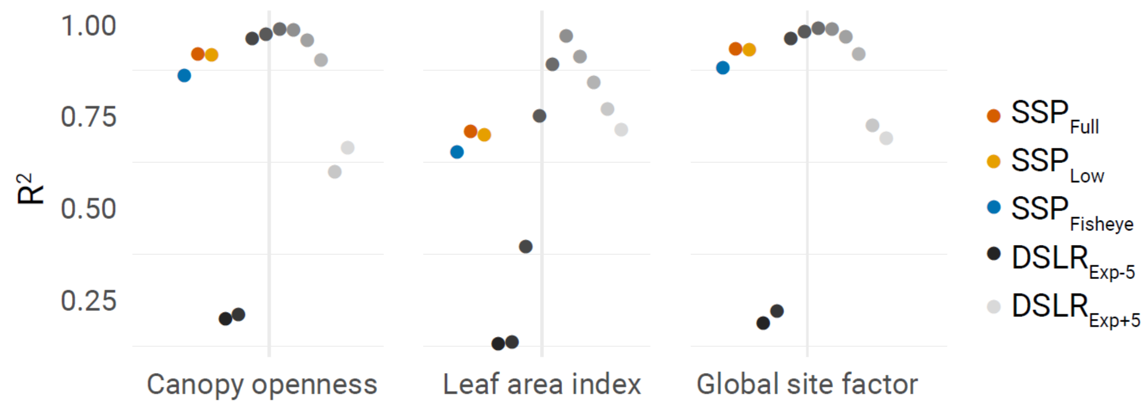

Figure S5. Coefficients of determination from independent OLS regression models predicting canopy structure and light environment values for reference (standard DSLR HP) from full resolution SSP HP (dark orange), low resolution SSP HP downsampled to match the standard DSLR resolution (light orange), fisheye HP (blue), and DSLR HP with exposure adjusted from +5 to -5 (light to dark).

Estimation of canopy clumping index

Methods

Canopy properties and clumping index were estimated by partitioning canopy gaps into within-canopy and between-canopy gaps (Chen and Cihlar, 1995) using a thresholding method derived from Alivernini *et al.* (2018).

Gap size was estimated using the Analyze Particles tool in ImageJ on inverted binary images output from Hemispherical 2.0 plugin. Gaps that greater than one standard error in excess of the mean of the distribution of gap sizes for an image were considered as large, between-canopy gaps. The proportion of total gap area (g_T) or large gap area (g_L) to circular image area (p_r) was used to calculate total gap fraction (GF_T) and large gap fraction (GF_L), respectively. Crown cover (CC), foliage cover (FC), crown porosity (CP), and clumping index (CI) were estimated (following Alivernini *et al.* (2018)) as:

$$CC = 1 - GF_L$$

$$FC = 1 - GF_T$$

$$CP = 1 - \frac{FC}{CC}$$

$$CI = \frac{(1 - CP) * ln(1 - FC)}{ln(CP) * FC}$$

Results

Table S3. Estimates of canopy properties from hemispherical photos captured at 72 sites using smartphone spherical panoramas (SSP) HP or DSLR HP, and the difference in estimates (SSP HP - DSLR HP). The mean value is shown followed by standard deviation in parentheses.

Method	Number of large gaps	GF_T	GF_L	CC	FC	CP	CI
SSP HP	2067 (897)	6.76 (5.34)	5.85 (5.06)	0.94 (0.05)	0.93 (0.05)	0.010 (0.004)	0.64 (0.05)
DSLR HP	292 (174)	5.56 (6.12)	4.89 (5.84)	0.95 (0.06)	0.94 (0.06)	0.007 (0.005)	0.66 (0.08)
Difference	1774 (806)	1.20 (1.75)	1.00 (1.56)	-0.01 (0.02)	-0.01 (0.02)	0.003 (0.003)	-0.02 (0.02)

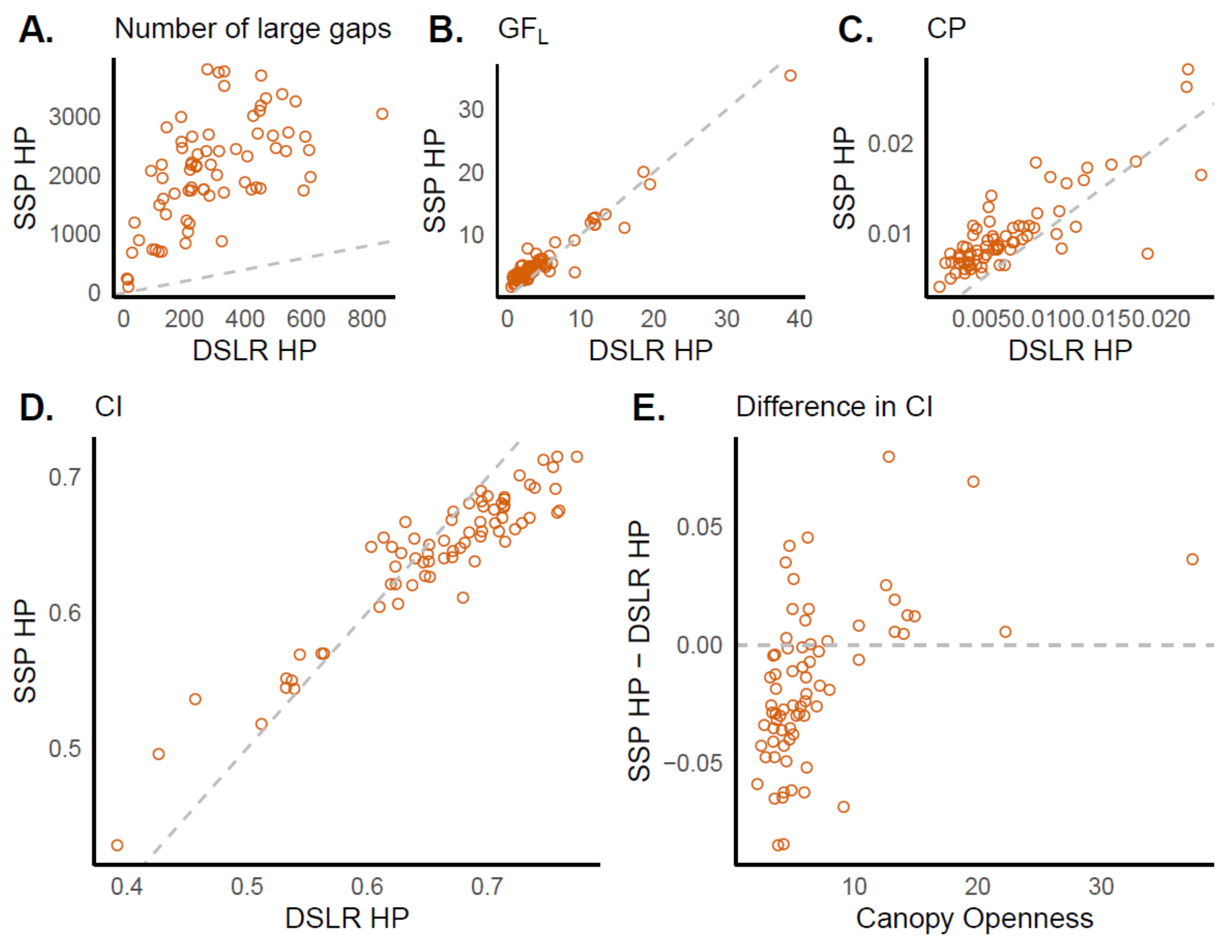

Figure S6. Comparison of canopy properties including the number of large (i.e. between-canopy) gaps (A), large gap fraction (B), canopy porosity (C), and clumping index (D) from hemispherical photos captured at 72 sites using DSLR HP or smartphone spherical panoramas (SSP) HP. The difference in clumping index estimated from images produced with SSP HP or DSLR HP relative to canopy openness is shown in E. The 1 to 1 line (dashed) is shown in all panels.

References:

Alvernini, A., Fares, S., Ferrara, C. & Chianucci, F. (2018). ‘An objective image analysis method for estimation of canopy attributes from digital cover photography’, *Trees*, 32, pp. 713-723.

Chen, J. M., and Cihlar, J. (1995). Plant canopy gap-size analysis theory for improving optical measurements of leaf-are index. *Applied Optics*, 34(27), 6211–6222.